Journal of Biosciences and Medicines, 2025, 13(11), 16-25
https://www.scirp.org/journal/jbm
ISSN Online: 2327-509X
ISSN Print: 2327-5081

Construction of Overexpression Vector for *Arabidopsis SOC3* and Its Transient Expression in *Nicotiana benthamiana*

Qiang Lin, Jiayu Zeng, Xiaoju Zhong, Zhuojun Li, Hongbin Zhang, Jianzhong Huang*

Department of Basic Medicine, Fuzhou Medical University (Formerly Known as the Fuzhou Medical College of Nanchang University), Fuzhou, China
Email: *huangjz@whu.edu.cn

How to cite this paper: Lin, Q., Zeng, J.Y., Zhong, X.J., Li, Z.J., Zhang, H.B. and Huang, J.Z. (2025) Construction of Overexpression Vector for *Arabidopsis SOC3* and Its Transient Expression in *Nicotiana benthamiana*. *Journal of Biosciences and Medicines*, **13**, 16-25.
https://doi.org/10.4236/jbm.2025.1311002

Received: September 20, 2025
Accepted: October 27, 2025
Published: October 30, 2025

Abstract

[**Objective**] To clone the TIR-NBS-LRR class *SOC3* gene in *Arabidopsis thaliana* and analyze its subcellular localization and function in both full-length and truncated fragments. [**Method**] Full-length *SOC3* and its segments cDNA were acquired through RT-PCR with mRNA isolated from leaves of *Arabidopsis*, and their localization and function in *Nicotiana benthamiana* were investigated employing Agrobacterium-mediated transient expression technology. [**Result**] Obtained the full-length cDNA of *SOC3, which encodes a 1049 amino acid polypeptide with a calculated molecular mass of* 118.57 kDa *and an isoelectric point of* 7.27. Subcellular localization studies revealed that *SOC3* and its TIR domain are located in the nucleus, cytoplasm, and cell membrane. In addition, *SOC3*-TIR alone triggers cell death in N. *benthamiana, which cannot be abolished by co-expression of EXO70B1.* [**Conclusion**] *SOC3* and SOC-TIR are both located in the plasma membrane, cytoplasm, and nucleus, and SOC-TIR domain has cell-death-inducing activity in *N. benthamiana.*

Keywords

Arabidopsis, TIR-NBS-LRR, Cell Death, *Nicotiana benthamiana*

1. Introduction

During the growth and development of plants, they are constantly threatened and challenged by various pathogenic microorganisms. To survive, plants have evolved two levels of immune systems [1]. The first level of immune response is initiated by pattern-recognition receptors (PRRs) on the cell surface that recognize pathogen-associated molecular patterns (PAMPs), known as PAMP-trig-

*Corresponding author.

gered immunity (PTI) [2]. Certain pathogens can overcome PTI through secreting effectors. Correspondingly, host plants utilize intracellular resistance (R) proteins to monitor effectors, thereby activating the second level of the immune system, namely effector-triggered immunity (ETI) [3]. ETI is more rapid and intense than PTI, and is often accompanied by visible cell death to limit the invasion of pathogens at the infection site, called hypersensitive response (HR) [4].

Cloning the plant R genes and clarifying its resistance mechanism is of great significance for deepening the understanding of resistance molecular mechanisms and improving agricultural production. In recent years, a large number of R genes have been cloned, with the largest category being R proteins encoding conserved motifs containing nucleotide binding sites and leucine-rich repeats (NBS-LRRs; NLRs). There are about 150 NLR genes in *Arabidopsis thaliana* [5]. Based on the N-terminal domain, plant NLRs are usually divided into three categories: CC (coiled-coil)-NBS-LRR (CNL), TIR (toll/interleukin-1 receptor)-NBS-LRR (TNL) and RPW8 (resistance to powdery mildew 8)-NBS-LRR (RNL) [6].

The CC domains or TIR domains of multiple NLRs, such as Sr33, Sr50, ZAR1, MLA10, RP1-D21 are enough to induce cell death after transient expression in leaves of *Nicotiana benthamiana* [7]-[11]. However, there are other NLRs, including RPM1, Rx, and RPS5, whose CC domains do not touch off cell death in *N. benthamiana* [12]-[14]. The subcellular localization patterns of NLRs are diverse. For example, RPM1 and RPS5 are localized on the plasma membrane [14] [15]. L6 and M proteins are localized on the Golgi and tonoplast, respectively [16]. RGA4 and RGA5 are mainly localized in the cytosol [17]. In addition, SNC1, Rx, and MLA10 exhibit a nucleo-cytoplasmic localization characteristic [7] [18] [19]. Different localizations of NLRs reflect their different activation mechanisms.

To investigate the role of NLR genes, this study cloned a TNL gene *SOC3* from wild-type *Arabidopsis*, conducted bioinformatics analysis on it, and successfully constructed an overexpression vector. Subsequently, the full-length *SOC3* and its truncated fragments were transiently expressed in *N. benthamiana*, providing a basis for further research on the biological function of the *SOC3* receptor.

2. Materials and Methods

2.1. Plant Materials and Growth Environment

N. benthamiana and *Arabidopsis* plants were grown in a growth chamber at 24˚C with a 16 h-light/8 h-dark photoperiod [20].

2.2. Arabidopsis RNA Extraction and cDNA Synthesis

Total RNAs were extracted from four-week-old leaves of *Arabidopsis* lines and the reverse transcription of RNAs was implemented through using Transcript One-step gDNA Removal and cDNA Synthesis SuperMix. All cDNAs were diluted to 100 ng/moL.

2.3. Construction of the Overexpression Vector

In order to acquire overexpression vectors containing full-length *SOC3* and its

truncated fragments separately, we first employed cDNA of wild-type *Arabidopsis* leaves as a template and amplified it by PCR. Conditions for the PCR amplification are: 36 cycles of a 30-second denaturation step at 94˚C, annealing at 56˚C for 30 seconds, and extension at 72˚C for 1 minute. Afterwards, we collected the above fragments separately and cloned them into modified pUC19. After extracting the plasmid, DNA sequencing was conducted, and finally the correct plasmid was ligated to the expression vector pEarleyGate101 fused with the YFP-HA tag utilizing gateway technology. Electro-transfer the expression plasmid into *Agrobacterium tumefaciens* strain GV3101.

2.4. Agrobacterium Transient Expression Assays

The Agrobacterium containing different constructs were cultured in LB medium containing kanamycin and rifampicin and grown overnight. Bacteria were collected by centrifugation and resuspended in infiltration medium [10 mM $MgCl_2$, 10 mM MES (pH 5.6), and 200 muM acetosyringone] at room temperature for 1 hour before injection into 4-week-old *N. benthamiana* leaves [21]. Each experiment was repeated at least three times and yielded similar results.

2.5. Subcellular Localization Observation

The YFP fluorescence was observed using a fluorescence microscope after infiltration for 48 hours. YFP was excited using the 514 nm laser line, and the emission was collected at 520 - 570 nm. All experiments were repeated at least three times to yield comparable results.

3. Results

3.1. Analysis of Physical and Chemical Properties and Structure Prediction of *SOC3* Protein

The *SOC3* belongs to TIR-NBS-LRR protein [22]. The basic physicochemical properties of the proteins encoded by the *SOC3* gene were analyzed using ProtParam (https://web.expasy.org/protparam/). The number of amino acid residues of the *SOC3* protein was 1049, the formula was $C_{5278}H_{8474}N_{1446}O_{1537}S_{56}$, the theoretical isoelectric point was 6.9, and the predicted molecular weight was 118.5 kDa, respectively. It is worth noting that the instability coefficient of the *SOC3* protein was 42.33, so *SOC3* belongs to the unstable proteins. The hydrophilicity/hydrophobicity of *SOC3* was analyzed using ExPASy-ProtScale (https://web.expasy.org/protscale/), revealing an uneven distribution of hydrophilic and hydrophobic amino acids across the sequence, with an average hydrophilicity index of -0.490, indicating it is a hydrophilic protein (**Figure 1(A)**). Signalp-5.0 (https://services.healthtech.dtu.dk/services/SignalP-5.0/) predicted that the *SOC3* protein does not possess signal peptides (**Figure 1(B)**). Using SWISS-MODEL (https://swissmodel.expasy.org/) predicts the three-dimensional structure of the *SOC3* protein (**Figure 1(C)**), and the crystal structure of *Arabidopsis* RPP1 protein (belonging to TNL protein) (7crc.1.B) was chosen as the template for *SOC3* protein with its sequence identity at 35.99%, GMQE (Global

Model Quality Estimate) score of 0.51, and QMEANDisCo (Qualitative Model Energy ANalysis DIStance COnstraint) global score of 0.54 ± 0.05.

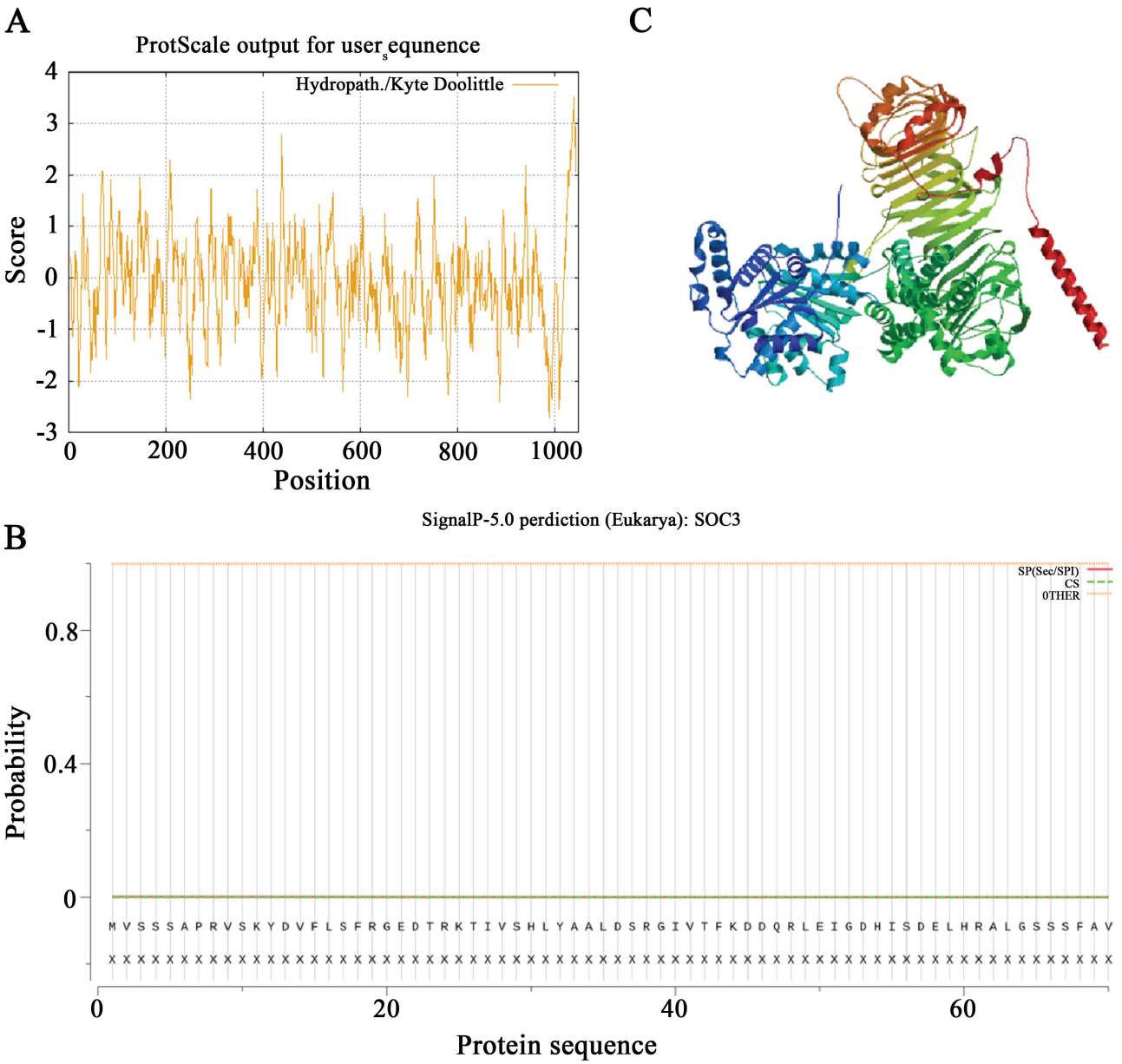

Figure 1. Bioinformatics analysis of *SOC3* protein. (A) Hydrophobicity prediction. (B) Protein signal peptide prediction. (C) The tertiary structure prediction of *SOC3* protein.

3.2. Construction of the *SOC3* Gene Plant Expression Vector

Based on gene annotation results and the reference sequence of *Arabidopsis SOC3* (AT1G17600; https://www.arabidopsis.org/), we designed the specific PCR primers (*SOC3*-F: 5'-CTCCGCGGCCGCCACCATGGTGTCCTCCTCTGCACC-3', *SOC3*-R: 5'-GGTCGGCGCGCCCCTTGAAAACACGCAGGAGTAAAATCAC-3'), to amplify the coding sequence of *SOC3*, which introduces a 15-bp overlap region with the modified cloning vector pUC19 (the gateway entry vector). The

results of agarose gel electrophoresis of the PCR amplification product are shown in Figure 2(A), and it was assembled using the ClonExpress II One Step Cloning Kit to construct the pUC19-*SOC3* plasmid. Furthermore, pUC19-*SOC3* was transformed into competent cells *E. coli*, and positive clones were identified through PCR verification using specific primers (501-F: 5'-TAACGCTAG-CATGGATGTTTTCC-3', 870-R: 5'-CAGAGCTGCCAGGAAACAGC-3') (Figure 2(B)). Selected clones underwent plasmid extraction, and sequencing results indicated that the amplified product is indeed the coding sequence of the *SOC3* gene. Then, the sequenced pUC19-*SOC3* plasmid was ligated to the destination binary overexpression vector pEarleyGate101 by LR reaction using the Gateway recombination system following the manufacturer's instruction, and the product was transformed into competent *E. coli* cells again. Positive monoclonals were obtained through PCR identification using specific primers (35S-F: 5'-ATGAC-GCACAATCCCACTATC-3', OCS-R: 5'-GCGCTCTATCATAGATGTCGC-TATAAAC-3') (Figure 2(C)), and the extracted plasmid was pEarleyGate101-*SOC3*-YFP-HA, which was used for subsequent transient expression analysis.

Following the same cloning method, we replaced specific PCR amplification primers and obtained plant overexpression vectors containing three domain fragments of the *SOC3* gene (TIR: 1-186 aa; NBS: 187-510 aa; LRR: 511-1049 aa) (COBALT: Multiple Alignment Tool), respectively.

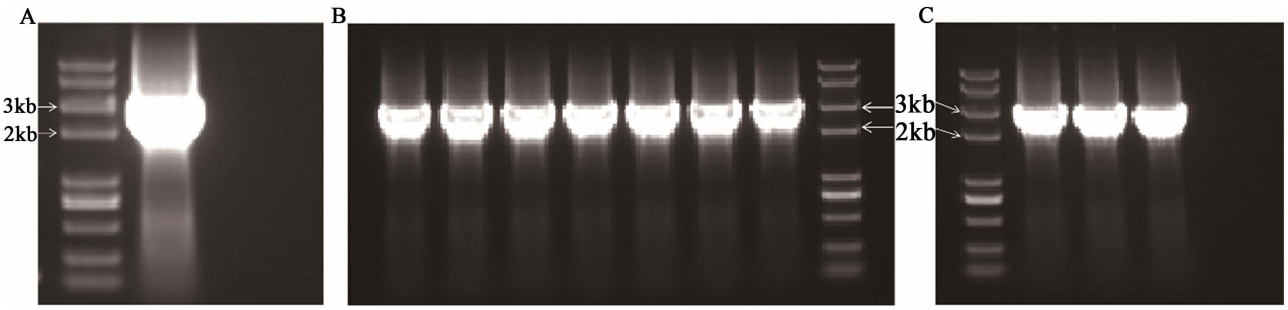

Figure 2. Construction of *SOC3* gene plant expression vector. (A) The full-length *SOC3* clone was amplified by PCR using cDNA as the template and the gene-specific primer pair. Use 1% agarose gel electrophoresis to check the purity and concentration of the DNA. (B) Fragment of the correct size was cloned into the modified pUC19 plasmid and the insert was verified by PCR and complete sequencing using vector primers and anticipated gene specific primers. (C) Connect the correctly sequenced pUC19-*SOC3* plasmid to the pEarletGate101 vector, validate the insert by PCR, and perform complete sequencing using vector primers and expected gene-specific primers.

3.3. *SOC3* Was Distributed in the Nucleus, Cytoplasm, and Plasma Membrane

The subcellular localization of proteins is closely related to their biological function [23]. To investigate the localization pattern of *SOC3* receptor, we electroporated the constructed plant overexpression vector into *Agrobacterium* strain GV3101 and used *Agrobacterium*-mediated transformation to transiently express the fusion protein in the leaves of *N. benthamiana*. The yellow fluorescence of the *SOC3*-YFP-HA fusion proteins was localized to the plasma membrane, cytoplasm and nucleus (Figure 3(A)). Ulteriorly, in *N. benthamiana* cells expressing *SOC3*-

TIR alone, fluorescence signal was observed in cytoplasm, plasma membrane and nucleus; while in *N. benthamiana* leaves expressing *SOC3*-NBS-YFP-HA and *SOC3*-LRR-YFP-HA, the fluorescence signal was mainly concentrated in the cytoplasm and plasma membrane (**Figure 3(B)**).

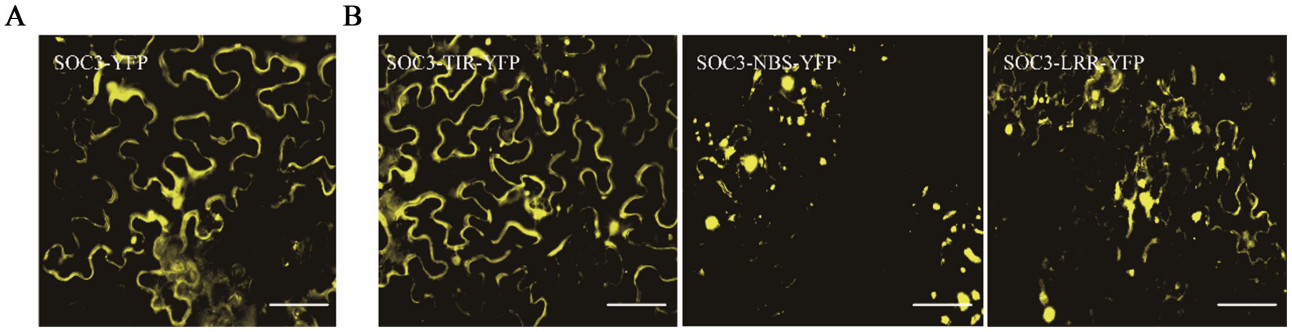

Figure 3. Subcellular localization of the full-length Rx1 and its three domains. (A) Localization pattern of *SOC3*-YFP-HA. Bar=50 mm. (B-D) Localization pattern of *SOC3*-TIR, *SOC3*-NBS, and *SOC3*-LRR. The YFP-HA-labeled protein was imaged by fluorescence microscopy in epidermal cells of transiently transformed *N. benthamiana* leaves. Images were taken 3 days after agroinfiltration. *SOC3*-TIR: bar=50 mm; both *SOC3*-NBS and *SOC3*-LRR: bar = 20 mm.

3.4. *SOC3*-TIR-Induced Cell Death in *N. benthamiana* Cannot Be Suppressed by Co-Expression with *EXO70B1*

We transiently expressed the full-length *SOC3* and its three domains in the leaves of *N. benthamiana*, respectively, and the results showed that *SOC3*-TIR alone triggers strong and rapid cell death. We detected that the expression levels of full-length and truncated *SOC3* were at comparable levels, ruling out the possibility that their functional differences were caused by changes in protein expression (data not displayed) (**Figure 4(A)**). Previous studies have shown that expression of TN2 in *N. benthamiana* induces cell death, which is suppressed by co-expression with *EXO70B1* [24]. Considering that *SOC3* interacts with TN2 in planta [22], we want to know whether *EXO70B1* could also inhibit cell death induced by *SOC3*-TIR in *N. benthamiana*. The results indicated that co-expression of *EXO70B1* cannot abolish the cell-death-inducing activity of *SOC3*-TIR (**Figure 4(B)**).

4. Discussion

The TIR domain of *SOC3* initiated cell death in *N. benthamiana*, but the TIR-NBS fragment cannot (**Figure 4(A)**), declaring that the NBS domain of *SOC3* suppressed the activation of TIR, and the intra-molecular interaction can regulate the activation of full-length *SOC3*. Previous studies have suggested that the TIR modules of some plant NLRs, such as L6^{TIR}, SNC1^{TIR}, and RPS4^{TIR}, can trigger cell death in *N. benthamiana* leaves, and these TIR domains exhibit NAD$^+$ cleavage activity. In NADases, a catalytic glutamate typically interacts with the C-2 and C-3 hydroxyl groups of the Namri bose in NAD$^+$ [25]. Mutation of the conserved catalytic glutamate in L6^{TIR}-YFP, SNC1^{TIR}-YFP, and RPS4^{TIR}-YFP abrogated effector-independent HR detected by transient expression [26]. In addition, Li *et al*. found

that TIR immune signaling is blocked by phosphorylation to maintain growth in plants and animals [27]. In the *SOC3*^{TIR} structure, E86 forms hydrogen bonds with the C-2 and C-3 hydroxyl groups of glycerol and also contains conserved serine residues. In this article, we demonstrated that the *SOC3*-TIR also has cell-death-inducing activity in plants. Future research should focus on determining whether the *SOC3*-TIR domain also has NAD^+ cleavage activity and whether mutated conserved serine residues can abolish its cell-death-inducing activity.

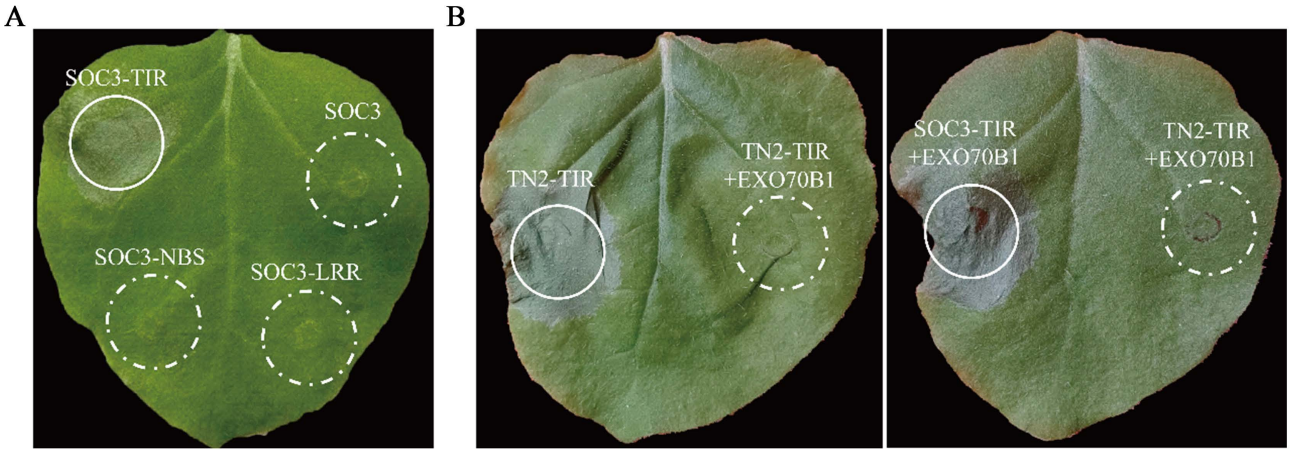

Figure 4. *SOC3*-TIR-triggered cell death in *N. benthamiana* cannot be abolished by co-expression with *EXO70B1*. (A) *SOC3*-TIR overexpression rapidly induced cell death (OD_{600} = 0.1). The image was recorded 48 h post infiltration (hpi). White solid line circles show cell death, while the white dashed line circles indicate no apparent cell death in the infiltrated area. (B) Co-expression of *EXO70B1* inhibited the hypersensitive response triggered by TN2-TIR instead of *SOC3*-TIR in *N. benthamiana* leaves (both TN2-TIR and *SOC3*-TIR: OD_{600} = 0.6). The image was recorded 72 hpi.

We observed that *SOC3* was distributed in the cell membrane, nucleus, and cytoplasm and was therefore a nucleoplasmic protein (**Figure 3(A)**). Due to the lack of a typical nuclear localization signal (NLS) sequence, NBS-LRR protein was previously believed to function in the cytoplasm. However, a number of studies have demonstrated that coordinated nucleo-cytoplasmic trafficking of plant NLRs is required for the full activation of defense responses, suggesting that a single NLR protein may activate distinct signaling pathways in the cytoplasm and nucleus. For example, *Arabidopsis* TNL protein RRS1-R interacts with the effector PopP2 of *Ralstonia solanacearum* in the nucleus, and forms a complex with the nuclear-expressed protein cysteine protease RD19 (Responsive Dehydration 19), initiating resistance to pathogens [28]. In addition, the recognition of barley disease resistance protein MLA10 and powdery mildew effector factor A10 induces MLA10 to bind to the transcription factor WRKY in the nucleus, initiating the disease resistance response. The co-expression of MLA10 fusion protein containing a nuclear export signal (NES) leads to the export of R protein to the extracellular space, resulting in the disappearance of resistance [29]. The potato Rx1, which confers extreme resistance to Potato virus X, is located both in the nucleus and cytoplasm. Manipulating the nucleocytoplasmic distribution of Rx1 or its elicitor revealed that Rx1 is activated in the cytoplasm and cannot be activated in the nucleus [18].

5. Conclusion

SOC3 and SOC-TIR are both located in the plasma membrane, cytoplasm, and nucleus, and SOC-TIR domain exhibits cell-death-inducing ability in *N. benthamiana*, which cannot be suppressed by co-expression of *EXO70B1*.

Acknowledgements

Our functional data are limited to the transient system of *N. benthamiana*, and confirmation in *Arabidopsis* remains a future objective.

Funding

This study received grant from the Science and Technology Research Project of Jiangxi Provincial Department of Education (GJJ2403304 and GJJ218112).

Conflicts of Interest

The authors declare that they have no conflicts of interest.

References

[1] Jones, J.D.G. and Dangl, J.L. (2006) The Plant Immune System. *Nature*, **444**, 323-329. https://doi.org/10.1038/nature05286

[2] Saijo, Y., Loo, E.P. and Yasuda, S. (2018) Pattern Recognition Receptors and Signaling in Plant–Microbe Interactions. *The Plant Journal*, **93**, 592-613. https://doi.org/10.1111/tpj.13808

[3] Remick, B.C., Gaidt, M.M. and Vance, R.E. (2023) Effector-Triggered Immunity. *Annual Review of Immunology*, **41**, 453-481. https://doi.org/10.1146/annurev-immunol-101721-031732

[4] Balint-Kurti, P. (2019) The Plant Hypersensitive Response: Concepts, Control and Consequences. *Molecular Plant Pathology*, **20**, 1163-1178. https://doi.org/10.1111/mpp.12821

[5] Jones, J.D.G., Vance, R.E. and Dangl, J.L. (2016) Intracellular Innate Immune Surveillance Devices in Plants and Animals. *Science*, **354**, aaf6395. https://doi.org/10.1126/science.aaf6395

[6] Wang, W., Feng, B., Zhou, J. and Tang, D. (2020) Plant Immune Signaling: Advancing on Two Frontiers. *Journal of Integrative Plant Biology*, **62**, 2-24. https://doi.org/10.1111/jipb.12898

[7] Bai, S., Liu, J., Chang, C., Zhang, L., Maekawa, T., Wang, Q., *et al.* (2012) Structure-function Analysis of Barley NLR Immune Receptor MLA10 Reveals Its Cell Compartment Specific Activity in Cell Death and Disease Resistance. *PLOS Pathogens*, **8**, e1002752. https://doi.org/10.1371/journal.ppat.1002752

[8] Baudin, M., Hassan, J.A., Schreiber, K.J. and Lewis, J.D. (2017) Analysis of the ZAR1 Immune Complex Reveals Determinants for Immunity and Molecular Interactions. *Plant Physiology*, **174**, 2038-2053. https://doi.org/10.1104/pp.17.00441

[9] Cesari, S., Moore, J., Chen, C., Webb, D., Periyannan, S., Mago, R., *et al.* (2016) Cytosolic Activation of Cell Death and Stem Rust Resistance by Cereal MLA-Family CC–NLR Proteins. *Proceedings of the National Academy of Sciences*, **113**, 10204-10209. https://doi.org/10.1073/pnas.1605483113

[10] Collier, S.M., Hamel, L. and Moffett, P. (2011) Cell Death Mediated by the N-Terminal Domains of a Unique and Highly Conserved Class of NB-LRR Protein. *Molecular Plant-Microbe Interactions*, **24**, 918-931. https://doi.org/10.1094/mpmi-03-11-0050

[11] Wang, G., Ji, J., EI-Kasmi, F., Dangl, J.L., Johal, G. and Balint-Kurti, P.J. (2015) Correction: Molecular and Functional Analyses of a Maize Autoactive NB-LRR Protein Identify Precise Structural Requirements for Activity. *PLOS Pathogens*, **11**, e1004830. https://doi.org/10.1371/journal.ppat.1004830

[12] Ade, J., DeYoung, B.J., Golstein, C. and Innes, R.W. (2007) Indirect Activation of a Plant Nucleotide Binding Site–Leucine-Rich Repeat Protein by a Bacterial Protease. *Proceedings of the National Academy of Sciences*, **104**, 2531-2536. https://doi.org/10.1073/pnas.0608779104

[13] El Kasmi, F., Chung, E., Anderson, R.G., Li, J., Wan, L., Eitas, T.K., *et al*. (2017) Signaling from the Plasma-Membrane Localized Plant Immune Receptor RPM1 Requires Self-Association of the Full-Length Protein. *Proceedings of the National Academy of Sciences*, **114**, E7385-E7394. https://doi.org/10.1073/pnas.1708288114

[14] Qi, D., DeYoung, B.J. and Innes, R.W. (2012) Structure-Function Analysis of the Coiled-Coil and Leucine-Rich Repeat Domains of the RPS5 Disease Resistance Protein. *Plant Physiology*, **158**, 1819-1832. https://doi.org/10.1104/pp.112.194035

[15] Gao, Z., Chung, E., Eitas, T.K. and Dangl, J.L. (2011) Plant Intracellular Innate Immune Receptor Resistance to pseudomonas Syringae pv. Maculicola 1 (RPM1) Is Activated at, and Functions on, the Plasma Membrane. *Proceedings of the National Academy of Sciences*, **108**, 7619-7624. https://doi.org/10.1073/pnas.1104410108

[16] Takemoto, D., Rafiqi, M., Hurley, U., Lawrence, G.J., Bernoux, M., Hardham, A.R., *et al*. (2012) N-Terminal Motifs in Some Plant Disease Resistance Proteins Function in Membrane Attachment and Contribute to Disease Resistance. *Molecular Plant-Microbe Interactions*, **25**, 379-392. https://doi.org/10.1094/mpmi-11-10-0272

[17] Césari, S., Kanzaki, H., Fujiwara, T., Bernoux, M., Chalvon, V., Kawano, Y., *et al*. (2014) The NB-LRR Proteins RGA4 and RGA5 Interact Functionally and Physically to Confer Disease Resistance. *The EMBO Journal*, **33**, 1941-1959. https://doi.org/10.15252/embj.201487923

[18] Slootweg, E., Roosien, J., Spiridon, L.N., Petrescu, A., Tameling, W., Joosten, M., *et al*. (2010) Nucleocytoplasmic Distribution Is Required for Activation of Resistance by the Potato NB-LRR Receptor Rx1 and Is Balanced by Its Functional Domains. *The Plant Cell*, **22**, 4195-4215. https://doi.org/10.1105/tpc.110.077537

[19] Xu, F., Cheng, Y.T., Kapos, P., Huang, Y. and Li, X. (2014) P-Loop-Dependent NLR SNC1 Can Oligomerize and Activate Immunity in the Nucleus. *Molecular Plant*, **7**, 1801-1804. https://doi.org/10.1093/mp/ssu097

[20] Huang, J., Jia, P., Zhong, X., Guan, X., Zhang, H. and Gao, Z. (2024) Ectopic Expression of the Arabidopsis Mutant L3 NB-LRR Receptor Gene in Nicotiana Benthamiana Cells Leads to Cell Death. *Gene*, **906**, Article 148256. https://doi.org/10.1016/j.gene.2024.148256

[21] Huang, J., Guan, X., Zhong, X., Jia, P., Zhang, H. and Ruan, H. (2024) Structural and Functional Insights into an Arabidopsis NBS-LRR Receptor in *Nicotiana benthamiana*. *American Journal of Molecular Biology*, **14**, 84-96. https://doi.org/10.4236/ajmb.2024.142007

[22] Liang, W., van Wersch, S., Tong, M. and Li, X. (2018) TIR-NB-LRR Immune Receptor SOC3 Pairs with Truncated TIR-NB Protein CHS1 or TN2 to Monitor the Homeostasis of E3 Ligase SAUL1. *New Phytologist*, **221**, 2054-2066.

[23] Tan, X., Chen, L., Chen, Y., Li, Y., Lu, L. and Li, E. (2025) The Small GTPases FoRab5, FoRab7, and FoRab8 Regulate Vesicle Transport to Modulate Vegetative Development and Pathogenicity in *Fusarium oxysporum* f. sp. Conglutinans. *Frontiers in Microbiology*, **16**, Article 1514092. https://doi.org/10.3389/fmicb.2025.1514092

[24] Wang, W., Liu, N., Gao, C., Rui, L. and Tang, D. (2019) The Pseudomonas Syringae Effector AvrPtoB Associates with and Ubiquitinates Arabidopsis Exocyst Subunit EXO70B1. *Frontiers in Plant Science*, **10**, Article 1027. https://doi.org/10.3389/fpls.2019.01027

[25] Shi, Y., Kerry, P.S., Nanson, J.D., Bosanac, T., Sasaki, Y., Krauss, R., *et al*. (2022) Structural Basis of SARM1 Activation, Substrate Recognition, and Inhibition by Small Molecules. *Molecular Cell*, **82**, 1643-1659.e10. https://doi.org/10.1016/j.molcel.2022.03.007

[26] Horsefield, S., Burdett, H., Zhang, X., Manik, M.K., Shi, Y., Chen, J., *et al*. (2019) NAD+Cleavage Activity by Animal and Plant TIR Domains in Cell Death Pathways. *Science*, **365**, 793-799. https://doi.org/10.1126/science.aax1911

[27] Li, J., Chen, S., Yu, B., Li, Q., Liu, R., Wang, Z., *et al*. (2025) TIR Immune Signalling Is Blocked by Phosphorylation to Maintain Plant Growth. *Nature Plants*, **11**, 1193-1204. https://doi.org/10.1038/s41477-025-02012-x

[28] Bernoux, M., Timmers, T., Jauneau, A., Brière, C., de Wit, P.J.G.M., Marco, Y., *et al*. (2008) RD19, Anarabidopsiscysteine Protease Required for RRS1-R–Mediated Resistance, Is Relocalized to the Nucleus by the *Ralstonia solanacearum* PopP2 Effector. *The Plant Cell*, **20**, 2252-2264. https://doi.org/10.1105/tpc.108.058685

[29] Shen, Q., Saijo, Y., Mauch, S., Biskup, C., Bieri, S., Keller, B., *et al*. (2007) Nuclear Activity of MLA Immune Receptors Links Isolate-Specific and Basal Disease-Resistance Responses. *Science*, **315**, 1098-1103. https://doi.org/10.1126/science.1136372